

COMSOL MULTIPHYSICS®

Proton Exchange Membrane Fuel Cell

SOLVED WITH COMSOL MULTIPHYSICS 3.5a

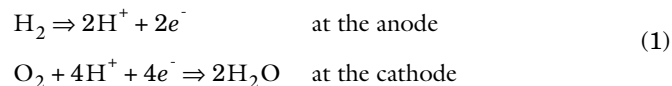
Proton Exchange Membrane Fuel Cell

Introduction

This example demonstrates the multiphysics modeling of a proton exchange membrane (PEM) fuel cell with an interdigitated flow field design. The model uses current balances, mass transport equations (Maxwell-Stefan diffusion for reactant, water and nitrogen gas), and momentum transport (gas flow) to simulate a PEM fuel cell's behavior.

One main candidate for clean high-efficiency power production in future cars is the PEM fuel cell. In a fuel cell-powered engine, the fuel is converted to electric energy through electrochemical reactions instead of combustion. An electric motor, which generally operates at a very high efficiency, powers the vehicle. The efficiency limitations (approximately 40%) of the Carnot cycle are overcome in this way, and the theoretical efficiency is substantially higher than that for combustion engines. Thus, a fuel cell-powered car can run for longer distances with the same amount of fuel compared to a conventional car. Carbon dioxide emissions are consequently lowered, because smaller amounts of fuel are consumed for the same distance traveled. In addition, the low temperatures in the process practically eliminate the production of NO_x and SO_x .

Figure 1 depicts the working principle of the PEM fuel cell. Oxidation of hydrogen and the reduction of oxygen takes place at the anode and cathode, respectively:



Electrons are released to an outer circuit at the anode, and they are received through the same circuit at the cathode. The electronic current is transported to and from the electrodes through the gas backing to the current collector and then to the outer electrical circuit. There is also an ionic current of protons running from the anode to the cathode through the electrolyte. Fuel cells are named after their electrolyte medium. In the PEM fuel cell, a polymeric proton exchange membrane serves as the electrolyte medium.

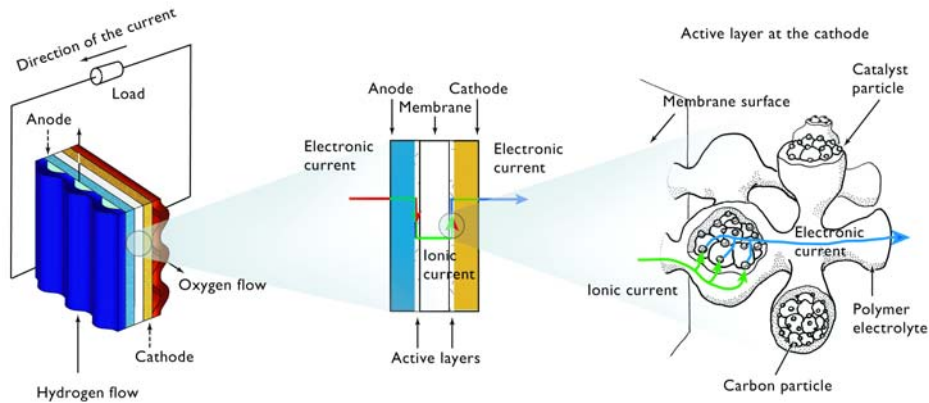


Figure 1: Working principle of a PEM fuel cell.

The PEM fuel cell electrodes are of the gas diffusion type. They consist of a supporting carbon structure with gas-filled pores (denoted gas backing) and a porous active layer that also contains the polymer electrolyte. The electrochemical reactions take place in the active layer, which contains a platinum catalyst. The gas diffusion electrodes are designed to maximize the specific area available for the reaction, maximize the distribution of reactant (that is, achieve a low gas-transport resistance), and minimize the resistance for the proton transport to and from the active sites at the electrodes.

Mathematical modeling is an important tool in the development of fuel cells. A combination of modeling and experiments has shown to lower costs and accelerate the pace of building prototypes and understanding these new systems. A number of models, each with a different focus and degree of complexity, have been presented in the literature (see References 1–4).

Model Definition

The modeled section of the fuel cell consists of three domains: an anode (Ω_a), a proton exchange membrane (Ω_m), and a cathode (Ω_c) as indicated in Figure 2. Each of the porous electrodes is in contact with an interdigitated gas distributor, which has an inlet

channel ($\partial\Omega_{a,inlet}$), a current collector ($\partial\Omega_{a,cc}$), and an outlet channel ($\partial\Omega_{a,outlet}$). The same notation is used for the cathode side.

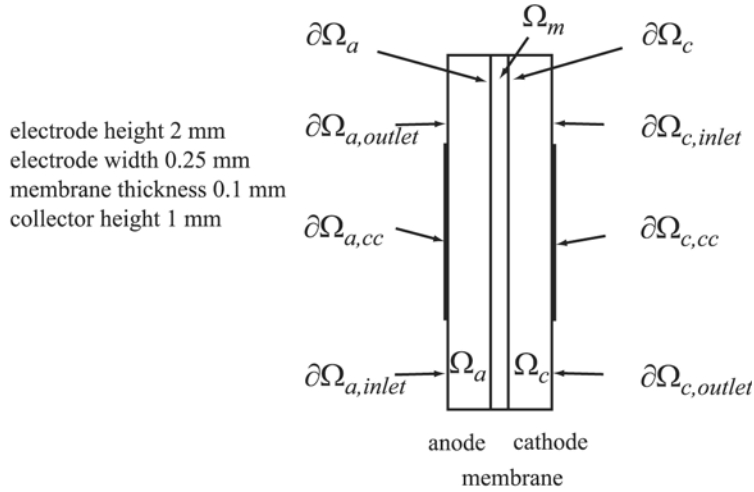


Figure 2: Model geometry with subdomain and boundary labels.

Humidified hydrogen and air are supplied to the inlet channels of the anode and cathode, respectively. Hydrogen reacts and is consumed at the anodic active layer to form protons that carry the ionic current to the cathode. Each proton is assumed to drag three molecules of water from the anode to the cathode. At the cathode, oxygen reacts together with the protons to form water at the active layer.

Both feed gases (humidified hydrogen and humidified air) are treated as ideal and are transported through diffusion and convection. The electrodes are treated as homogeneous porous media with uniform morphological properties such as porosity and permeability. The gas within each of the electrodes exists as a continuous phase so Darcy's law applies.

An agglomerate model describes the electrode reactions in the active catalyst layers. The agglomerates consist of catalyst and carbon particles embedded in polymer electrolyte. The equations for the agglomerate model originate from the analytical solution of a diffusion-reaction problem in a spherical porous particle (References 5 and 6). At the anodic active catalyst layer, hydrogen is the diffusing and reacting species in the agglomerates, while oxygen is the diffusion and reacting species in the agglomerates at the cathode. An agglomerate model of the cathodic active catalyst layer of a PEM fuel cell has been presented by Broka and others (Ref. 7 and Ref. 8).

CHARGE BALANCES

A Conductive Media DC application mode describes the potential distributions in the three subdomains using the following equations:

$$\begin{aligned} \nabla \cdot (-\kappa_{s, \text{eff}} \nabla \phi_s) &= 0 & \text{in } \Omega_a \\ \nabla \cdot (-\kappa_{m, \text{eff}} \nabla \phi_m) &= 0 & \text{in } \Omega_m \\ \nabla \cdot (-\kappa_{s, \text{eff}} \nabla \phi_s) &= 0 & \text{in } \Omega_c \end{aligned} \quad (2)$$

Here $\kappa_{s, \text{eff}}$ is the solid-phase effective electronic conductivity (S/m) and $\kappa_{m, \text{eff}}$ is the membrane ionic conductivity (S/m). The potential (V) in the electrode phases is denoted by ϕ_s and that in the membrane by ϕ_m .

This example models the active layer of the two electrodes as boundaries. This means that you treat the charge-transfer current density expression, generally described using the Butler-Volmer electrochemical kinetic expression, as a boundary condition.

For the electrolyte potential equation, this results in a condition where the inward normal ionic current densities at the anode and cathode boundaries, i_a and i_c , are specified according to the equation

$$i_e = L_{\text{act}} (1 - \varepsilon_{\text{mac}}) j_{\text{agg}, e} \quad (3)$$

where the index e stands for “a” (anode) or “c” (cathode). Further, L_{act} is the active layer’s thickness (m), ε_{mac} its porosity (the macroscopic porosity), and $j_{\text{agg}, a}$ and $j_{\text{agg}, c}$ are the current densities given by the agglomerate model.

AGGLOMERATE MODEL FOR ANODE AND CATHODE

The agglomerate model describes the current density in an active layer consisting of agglomerates of ionic conductor material and electrically conducting particles covered partially with catalyst. The local current density can be expressed analytically by solving a combination of the diffusion equation and the Butler-Volmer electrode kinetic equation for an agglomerate with constant electric and ionic potentials. The resulting equations for the current density in the anode and cathode are (Ref. 7)

$$j_{\text{agg}, e} = -6n_e F \left(\frac{D_{\text{agg}}}{R_{\text{agg}}^2} \right) (1 - \lambda_e \coth \lambda_e) \beta_e \quad (4)$$

where, again, the index e stands for “a” (anode) or “c” (cathode), and

$$\lambda_a = \sqrt{\frac{i_{0a} S R_{agg}^2}{2F c_{H_2, ref} D_{agg}}} \quad \lambda_c = \sqrt{\frac{i_{0c} S R_{agg}^2}{4F c_{O_2, ref} D_{agg}} \exp\left(-\frac{F}{2RT} \eta_c\right)} \quad (5)$$

$$\beta_a = \left[c_{H_2, ref} - c_{H_2, ref} \exp\left(\frac{-2F}{RT} \eta_a\right) \right] \quad \beta_c = c_{O_2, agg} \quad (6)$$

In these equations, D_{agg} is the agglomerate gas diffusivity (m^2/s), R_{agg} is the agglomerate radius (m), n_e is a “charge transfer” number (1 for the anode and -2 for the cathode), S is the specific area of the catalyst inside the agglomerate ($1/m$), and F is Faraday’s constant (C/mol). Furthermore, $c_{i, ref}$ are the reference concentrations of the species (mol/m^3), $c_{i, agg}$ are the corresponding concentrations in the agglomerate surface (mol/m^3), i_{0a} and i_{0c} are the exchange current densities (A/m^2), R is the gas constant, T is the temperature (K), and the overvoltages at the anode and the cathode are given by

$$\eta_a = \phi_s - \phi_m - E_{eq, a} \quad \eta_c = \phi_s - \phi_m - E_{eq, c} \quad (7)$$

where E_{eq} (V) denotes the equilibrium voltage.

You set the anodic and cathodic reference states equal to the molar fractions at the inlet channels of the anode and cathode, respectively, at 1 atm. The dissolved hydrogen and oxygen concentrations at the surface of the agglomerates are related to the molar fractions of the respective species in the gas phase through Henry’s law

$$c_{agg, H_2} = \frac{P_H x_H}{K_H} \quad (8)$$

$$c_{agg, O_2} = \frac{P_O x_O}{K_O}$$

where K is Henry’s constant ($Pa \cdot m^3/mol$).

CHARGE BALANCES, CONTINUED

For the electric potential, the electrode boundary conditions are identical, setting the boundary normal current density but using the opposite sign. In addition, the potential difference between the cathode and anode current collectors corresponds to the total cell voltage. Choose the potential at the anode current collector as the reference level by setting it to zero. Then the total cell voltage serves as the boundary condition at the cathode current collector:

$$\begin{aligned}\phi_s &= 0 & \text{at } \partial\Omega_{a,cc} \\ \phi_s &= V_{\text{cell}} & \text{at } \partial\Omega_{c,cc}\end{aligned}\quad (9)$$

For the other boundaries you have electric insulation boundary conditions.

POROUS MEDIA FLUID FLOW

To model the gas flows in the gas backings, this example uses the Darcy's Law application mode. The gas velocity is given by the continuity equation according to

$$\nabla \cdot (\rho \mathbf{u}) = 0 \quad \text{in } \Omega_a \text{ and } \Omega_c. \quad (10)$$

where ρ is the mixture density of the gas phase (kg/m^3) and \mathbf{u} denotes the gas velocity (m/s). Darcy's law for porous media states that the gradient of pressure, the viscosity of the fluid, and the structure of the porous media determine the velocity:

$$\mathbf{u} = -\frac{k_p}{\eta} \nabla p \quad (11)$$

Here k_p denotes the electrode's permeability (m^2), η represents the gas viscosity ($\text{Pa}\cdot\text{s}$), and p is the pressure (Pa). The ideal gas law gives the gas phase's mixture density, ρ :

$$\rho = \frac{p}{RT} \sum_i M_i x_i \quad (12)$$

In this equation, R denotes the gas constant ($\text{J}/(\text{mol}\cdot\text{K})$), T is the temperature (K), M is the molar mass (kg/mol), and x is the mole fraction.

At the inlets and outlets you specify the pressure:

$$\begin{aligned}p &= p_{a, \text{in}} & \text{at } \partial\Omega_{a, \text{inlet}} \\ p &= p_{\text{ref}} & \text{at } \partial\Omega_{a, \text{outlet}} \\ p &= p_{c, \text{in}} & \text{at } \partial\Omega_{c, \text{inlet}} \\ p &= p_{\text{ref}} & \text{at } \partial\Omega_{c, \text{outlet}}\end{aligned}\quad (13)$$

At the electrode boundary for the anode and cathode, the gas velocity is calculated from the total mass flow given by the electrochemical reaction rate according to

$$-\mathbf{n} \cdot \mathbf{u}|_{\text{anode}} = \frac{j_{\text{anode}}}{\rho F} \left(\frac{M_{\text{H}_2}}{2} + \lambda_{\text{H}_2\text{O}} M_{\text{H}_2\text{O}} \right) \quad (14)$$

$$-\mathbf{n} \cdot \mathbf{u}|_{\text{cathode}} = \frac{J_{\text{cathode}}}{\rho F} \left[\frac{M_{\text{O}_2}}{4} + \left(\frac{1}{2} + \lambda_{\text{H}_2\text{O}} \right) M_{\text{H}_2\text{O}} \right]. \quad (15)$$

Combined with these boundary conditions, Darcy's law determines the gas flow velocity and preserves the total mass conservation in the anode and cathode gas backing.

MAXWELL-STEFAN MASS TRANSPORT

The model takes into account two species in the anode— H_2 and H_2O —and three at the cathode— O_2 , H_2O , and N_2 . The model uses one instance of the Maxwell-Stefan Diffusion and Convection application mode for each electrode. Maxwell-Stefan multicomponent diffusion is governed by the equations

$$\begin{aligned} \frac{\partial}{\partial t} \rho w_i + \nabla \cdot \left[-\rho w_i \sum_{j=1}^N D_{ij} \left\{ \frac{M}{M_j} \left(\nabla w_j + w_j \frac{\nabla M}{M} \right) + (x_j - w_j) \frac{\nabla p}{p} \right\} + \right. \\ \left. w_i \rho \mathbf{u} + D_i^T \frac{\nabla T}{T} \right] = R_i \end{aligned} \quad (16)$$

which the software solves for the mass fractions, w_i . This particular PEM fuel cell model assumes that the temperature-driven diffusion is insignificant and sets the source term, R , to zero. For the cathode gas, with three species (oxygen = 1, water = 2, nitrogen = 3), the mass transport is described by the following three equations together with Darcy's law, describing the flow rate:

$$\nabla \cdot \left\{ -\rho w_1 \sum_j [D_{1j} (\nabla x_j + (x_j - w_j) (\nabla p / p))] \right\} = -(\rho \mathbf{u} \cdot \nabla w_1) \quad (17)$$

$$\nabla \cdot \left\{ -\rho w_2 \sum_j [D_{2j} (\nabla x_j + (x_j - w_j) (\nabla p / p))] \right\} = -(\rho \mathbf{u} \cdot \nabla w_2) \quad (18)$$

$$w_3 = 1 - w_1 - w_2 \quad (19)$$

Here p is the pressure (Pa), T is the temperature (K), and \mathbf{u} is the velocity (m/s). The density of the mixture is given by Equation 12. The Maxwell-Stefan diffusivity matrix, D_{ij} (m^2/s), is calculated from the binary diffusivities you specify in the application mode.

The feed-gas mass fractions are specified at the inlets. At the outlets, convective flux boundary conditions are applied, meaning that the flux is convection dominated. At

the electrode-membrane boundary, the mass fluxes of hydrogen in the cathode, and of oxygen and water in the cathode, are determined by the electrochemical reaction rate:

$$-\mathbf{n} \cdot \mathbf{N}_{\text{H}_2}|_{\text{anode}} = \frac{j_{\text{anode}}}{2F} M_{\text{H}_2} \quad (20)$$

$$-\mathbf{n} \cdot \mathbf{N}_{\text{O}_2}|_{\text{cathode}} = \frac{j_{\text{cathode}}}{4F} M_{\text{O}_2} \quad (21)$$

$$-\mathbf{n} \cdot \mathbf{N}_{\text{H}_2\text{O}}|_{\text{cathode}} = \frac{j_{\text{cathode}}}{F} \left(\frac{1}{2} + \lambda_{\text{H}_2\text{O}} \right) M_{\text{H}_2\text{O}} \quad (22)$$

Results and Discussion

Figure 3 shows the current distribution in the PEM fuel cell. There are significant current spikes present at the corners of the current collectors.

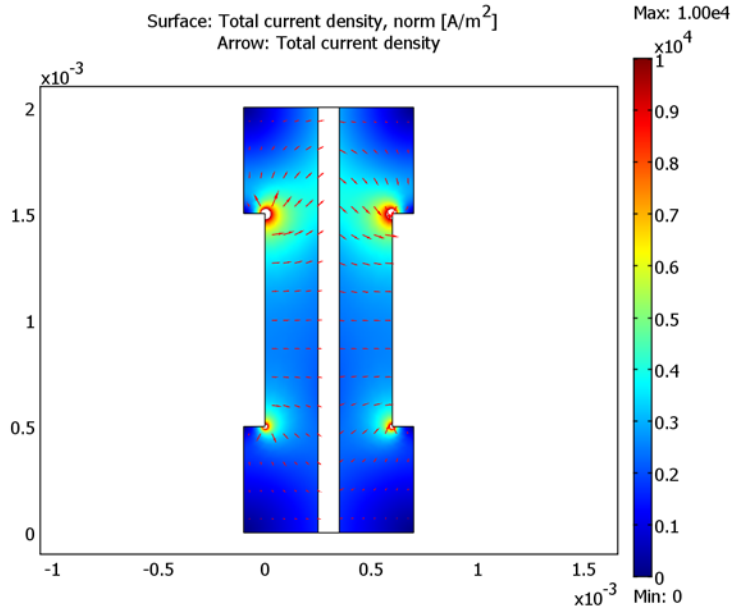


Figure 3: Current density (surface plot) and current vector field (arrow plot) in the fuel cell operating at 0.7 V. The anode is on the left and the cathode is on the right

To further analyze the cell's behavior, plot the current density at the active layer as a function of cell height (y) as in Figure 4.

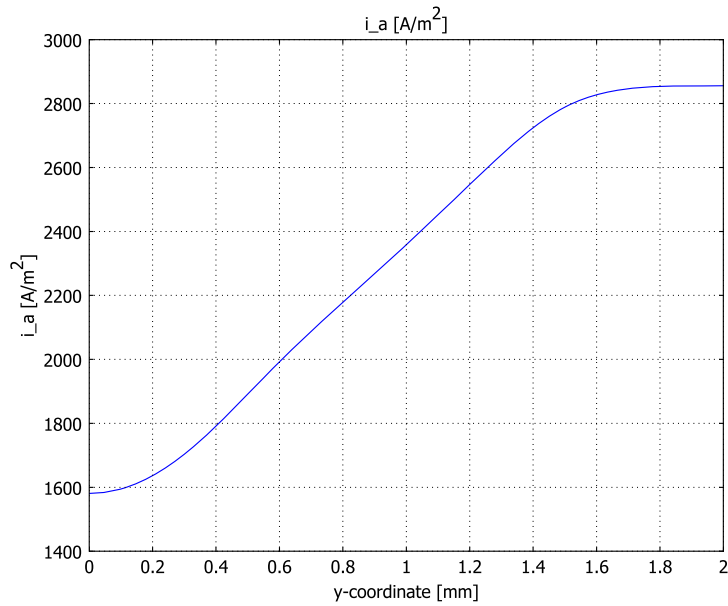


Figure 4: Current-density distribution at the active layer at the anode.

The current density is uneven with the highest density in the cell's upper region. This means that the oxygen-reduction reaction rate in the cathode determines the current-density distribution. The maximum current density arises close to the air inlet.

The convective fluxes generally dominate mass transport in the cell. To study the convective effects, plot the velocity field as in Figure 5.

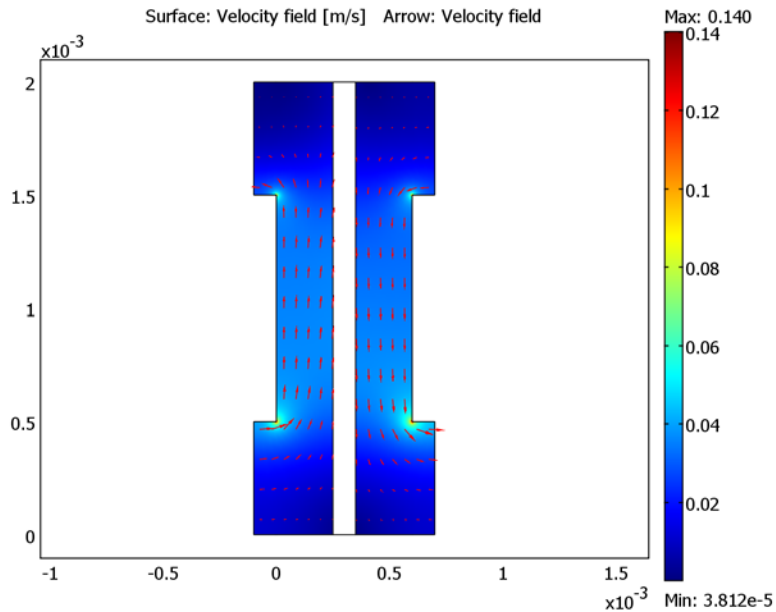


Figure 5: Gas velocity field in the anode and cathode compartments.

The flow-velocity magnitude attains its highest values at the current collector corners.

Figure 6 shows the reactant (oxygen and hydrogen) weight fractions in the cathode and anode gases. Surprisingly, the hydrogen fraction increases as the anode gas flows from the inlet (at the bottom) to the outlet (at the top). This is the result of the electroosmotic drag of water through the membrane, which results in a higher flux than the consumption of hydrogen. This means that the resulting convective flux of anode gas towards the membrane causes the weight fraction of hydrogen to go up. In the cathode gas, there is an expected decrease in oxygen content along the flow direction.

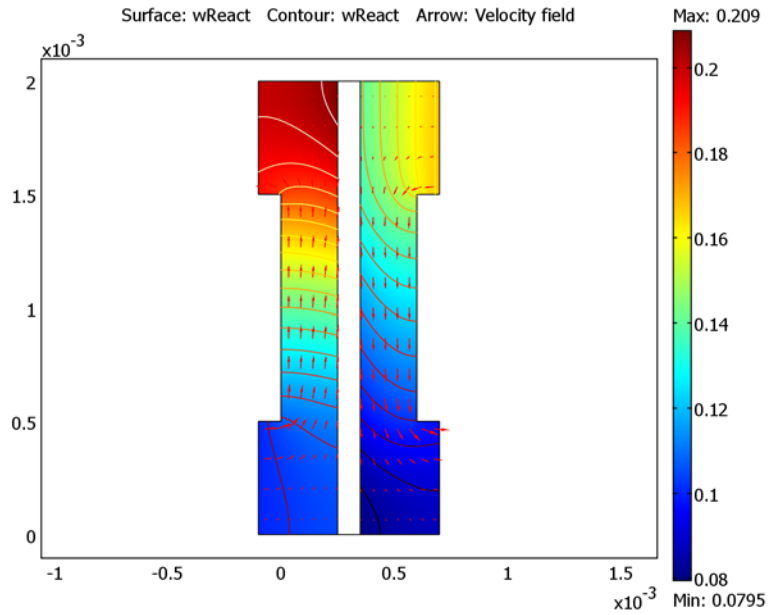


Figure 6: Reactant mass fractions, normalized by their inlet values, on the anode side (left) and cathode side (right). The reactant in the anode is hydrogen and that in the cathode is oxygen.

Although oxygen consumption is small, the concentration overvoltage in the agglomerates gives a substantial contribution to the concentration overvoltage. A small change in the oxygen flow gives a substantial change in cell polarization.

Figure 7 depicts the water mass fraction in the anode and cathode gases as well as the diffusive flux of water in the anode. It is apparent that water is transported through both diffusion and convection to the membrane on the anode side. The results show a minimum occurring in the upper corner of the membrane on the anode side. This is known to limit fuel cell performance. If the anode gas becomes too dry, the membrane dries out, resulting in decreasing ionic conductivity and the cell subsequently fails.

On the other hand, on the cathode side water levels increase with the direction of flow, and a local maximum in water current occurs in the lower corner to the membrane. This might also be critical because water droplets can clog the pores and effectively hinder gas transport to the active layer.

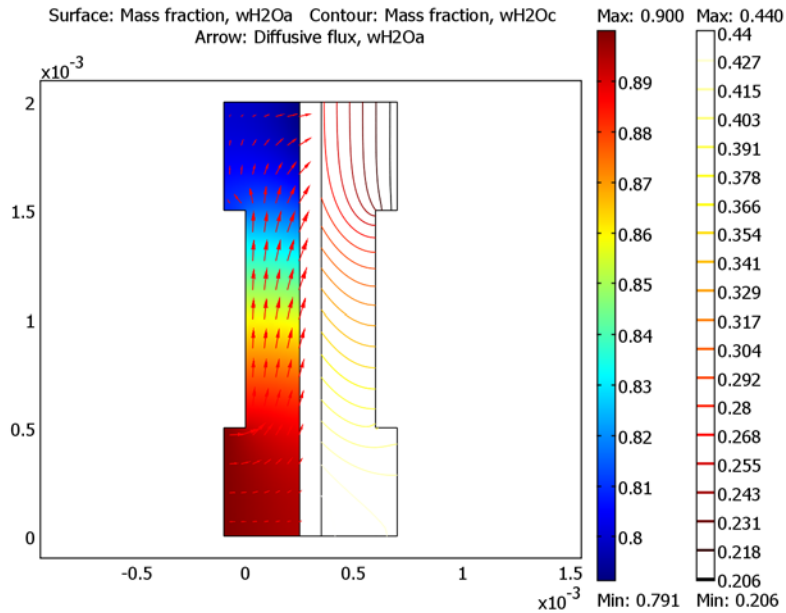


Figure 7: Water mass fraction in the anode (left, surface plot) and the cathode (right, contour plot). The arrows visualize the diffusive flux vector field on the anode side.

References

1. W. He, J.S. Yi, and T.V. Nguyen, “Two-Phase Flow Model of the Cathode of PEM Fuel Cells Using Interdigitated Flow Fields,” *AIChE J.*, vol. 46, pp. 2053–2063, 2000.
2. C. Marr and X. Li, “Composition and Performance Modelling of Catalyst Layer in a Proton Exchange Membrane Fuel Cell,” *J. Power Sources*, vol. 77, pp. 17–27, 1999.
3. P. Futerko and I.-M. Hsing, “Two-Dimensional Finite Element Method Study of the Resistance of Membranes in Polymer Electrolyte Fuel Cells,” *Electrochimica Acta*, vol. 45, pp. 1741–1751, 2000.
4. D.M. Bernardi and M.W. Verbrugge, “Mathematical Model of a Gas Diffusion Electrode Bonded to a Polymer Electrolyte,” *AIChE J.*, vol. 37, pp. 1151–1163, 1991.
5. H. Scott Fogler, *Elements of Chemical Reaction Engineering*, 3rd ed., Prentice Hall, 1999.

6. R. B. Bird, W. E. Stewart, and E. N. Lightfoot, *Transport Phenomena*, John Wiley & Sons, 1960.
7. K. Broka and P. Ekdunge, *J. Appl. Electrochem.*, vol. 27, p. 281, 1997.
8. K. Dannenberg, P. Ekdunge and, G. Lindbergh, *J. Appl. Electrochem.*, vol. 30, p. 1377, 2000.